PC3236 Project: Images of Schwarzschild Black Holes and their Accretions Disks

Fan Zeyu
A0211704W
31 Mar 2021

1 INTRODUCTION

We simulate how a black hole and its accretion disk would appear visually to a distant observer. Modelling the accretion disk as an ideal blackbody, we find the colour perceived by individual pixels of an imaginary camera via tracking the trajectory of a photon, considering the temperature of the disk as well as gravitational and relativistic redshift.

While the accretion disks of most black holes would have temperatures of around millions of Kelvins, we investigate the visual appearance of accretion disks with lower temperatures where the blue/redshift would cause noticeable differences in colour (at 1000-10000K).

In the images produced, we simulated a black hole with mass equal to Sagittarius A*, the supermassive black hole at the center of the Milky Way Galaxy, with an accretion disk of radius 10 times the Schwarzschild radius.

2 EQUATIONS AND PARAMETERS

2.1 *Trajectory of a photon*

The trajectory of a photon in its orbital plane is described by the below 2nd order ODE, under the Schwarzchild metric:

$$\frac{d^2u}{d\theta^2} + u = \frac{3GMu^2}{c^2} \qquad \textbf{Equation 1.}$$

Where $u = 1/r$, with standard polar coordinates.

2.2 *Parameterising the black hole and accretion disk*

For a standard Schwarzchild black hole, the event horizon is given by its Schwarzchild radius r_s:

$$r_s = \frac{2GM}{c^2}$$

Centering our black hole at the origin, the event horizon can be parameterised as the surface of a sphere with radius r_s. As for the accretion disk, we shall model it as a thin, uniform, opaque disk

of particles in circular motion around the black hole. Since the innermost stable circular orbit in the Schwarzschild metric[1] is at $r = 3r_s$, we assume that there is negligible matter in the volume for $r_s < r < 3r_s$, the disk can be parameterised as a surface on the x-y plane by:

$$\begin{pmatrix} r\cos\phi \\ r\sin\phi \\ 0 \end{pmatrix} \text{ for } 3r_s < r \leq R_{disk},\, 0 \leq \phi \leq 2\pi$$

For the observer to observe an inclined accretion disk rather than straight on or from the top, we rotate the accretion disk while positioning our observer on the z-axis. Since the black hole is spherical, it is invariant under rotation. Thus we only apply the transformation matrix corresponding to a rotation of α radians about the y-axis to the accretion disk:

$$\begin{pmatrix} \cos\alpha & 0 & \sin\alpha \\ 0 & 1 & 0 \\ -\sin\alpha & 0 & \cos\alpha \end{pmatrix} \begin{pmatrix} r\cos\phi \\ r\sin\phi \\ 0 \end{pmatrix} = \begin{pmatrix} r\cos\phi\cos\alpha \\ r\sin\phi \\ -r\cos\phi\sin\alpha \end{pmatrix} \text{ for } 3r_s < r \leq R_{\text{disk}},\, 0 \leq \phi \leq 2\pi$$

2.3 *Calculating the redshift*

The total redshift on a photon emitted from a certain point on the accretion disk is the product of gravitational redshift and the relativistic Doppler redshift; the cosmological redshift will be approximately constant over all regions of the accretion disk when the distance from the black hole is much larger than the radius of the accretion disk. It will be trivial to apply this redshift factor on top of the simulated values, and as such will be left out of the simulation. Thus, for an observer a large distance from the black hole, the simulated redshift will be given by:

$$\begin{aligned} \frac{\lambda_\infty}{\lambda_{\text{emitted}}} &= (1+z)_{\text{gravitational}}(1+z)_{\text{Doppler}} \\ &= \left(\frac{1}{\sqrt{1+\frac{r_s}{r}}}\right)\left(\frac{1+\beta\cos\psi}{\sqrt{1-\beta^2}}\right) \end{aligned} \qquad \textbf{Equation 2.}$$

Where r is the radius from which the photon is emitted from the disk, β ratio of v/c for the particle, and ψ the angle between $\vec{v}$ and the velocity vector of the photon. To find v, we assume a particle on the accretion disk is in circular orbit , which will be given by:

$$v = \sqrt{\frac{GM}{r - r_s}}$$

From spherical coordinates, the velocity vector of the photon can be found in terms of Cartesian coordinates ($\hat{e}_\phi$ element is 0 as $\dot{\phi}$ is 0):

$$\begin{aligned}\vec{v}_{\text{photon}} &= -\vec{v}_{\text{ray}} \\ &= -\frac{dr}{d\theta}\dot{\theta}\hat{e}_r - r\dot{\theta}\hat{e}_\theta \\ &= -\dot{\theta}\begin{pmatrix}(r\cos\theta + \frac{dr}{d\theta}\sin\theta)\cos\phi \\ (r\cos\theta + \frac{dr}{d\theta}\sin\theta)\sin\phi \\ -r\sin\theta + \frac{dr}{d\theta}\cos\theta\end{pmatrix}\end{aligned}$$

Which is equal in magnitude to c, which means $c = \dot{\theta}\sqrt{r^2 + \left(\frac{dr}{d\theta}\right)^2}$.

Prior to rotation about the y-axis, a particle on the accretion disk has velocity vector $\vec{v}_{\text{disk}} = v_0\hat{e}_\phi = v_0(-sin\phi\hat{e}_x + cos\phi\hat{e}_y)$. By the same rotation about y-axis applied to the black hole, this becomes:

$$\begin{aligned}\vec{v}_{\text{disk}} &= v\begin{pmatrix}\cos\alpha & 0 & \sin\alpha \\ 0 & 1 & 0 \\ -\sin\alpha & 0 & \cos\alpha\end{pmatrix}\begin{pmatrix}-\sin\phi \\ \cos\phi \\ 0\end{pmatrix} \\ &= v\begin{pmatrix}-\sin\phi\cos\alpha \\ \cos\phi \\ \sin\phi\sin\alpha\end{pmatrix}\end{aligned}$$

The cosine of the angle between $\vec{v}_{photon}$ and $\vec{v}_{disk}$ can thus be found as:

$$\begin{aligned}\cos\psi &= \frac{\vec{v}_{\text{photon}}\cdot\vec{v}_{\text{disk}}}{|\vec{v}_{\text{photon}}||\vec{v}_{\text{disk}}|} \\ &= \frac{\vec{v}_{\text{photon}}\cdot\vec{v}_{\text{disk}}}{vc} \\ &= -\frac{\sin\phi}{\sqrt{r^2 + \left(\frac{dr}{d\theta}\right)^2}}\left(\left(r\cos\theta + \frac{dr}{d\theta}\sin\theta\right)(1-\cos\alpha)\cos\phi + \left(-r\sin\theta + \frac{dr}{d\theta}\cos\theta\right)\sin\alpha\right)\end{aligned}$$

2.4 *Color of emitted light from accretion disk*

The spectrum of emitted light from an ideal blackbody at temperature T, which we shall model our accretion disk as, is described by Planck's Law:

$$B(\lambda, T) = \frac{2\pi hc^2}{\lambda^5}\frac{1}{e^{hc/\lambda k_B T} - 1}$$

To convert the spectrum to values of red, green, blue produced by a computer screen and visible to a human eye, the CIE colour matching functions are used to generate the parameters X, Y, Z in

the CIE 1931 XYZ colour space[2], and then converted to RGB values. Redshift is accounted for by having the emission spectra shifted by a factor of $(1+z)'$, the total redshift factor.

$$X(T) = \int_0^\infty \bar{x}(\lambda) B(\lambda/(1+z)', T) d\lambda$$
$$Y(T) = \int_0^\infty \bar{y}(\lambda) B(\lambda/(1+z)', T) d\lambda$$
$$Z(T) = \int_0^\infty \bar{z}(\lambda) B(\lambda/(1+z)', T) d\lambda$$

Where the colour matching functions are approximated by combinations of a piecewise Gaussian function $g(x)$ (units in Angstroms):

$$g(x; \alpha, \mu, \sigma_1, \sigma_2) = \begin{cases} \alpha \exp\left(\frac{(x-\mu)^2}{-2\sigma_1^2}\right) & x < \mu \\ \alpha \exp\left(\frac{(x-\mu)^2}{-2\sigma_2^2}\right) & \text{otherwise} \end{cases}$$

$$\bar{x}(\lambda) = g(\lambda; 1.056, 5998, 379, 310) + g(\lambda; 0.362, 4420, 160, 267) + g(\lambda; -0.065, 5011, 204, 262)$$
$$\bar{y}(\lambda) = g(\lambda; 0.821, 5688, 469, 405) + g(\lambda; 0.286, 5309, 163, 311)$$
$$\bar{z}(\lambda) = g(\lambda; 1.217, 4370, 118, 360) + g(\lambda; 0.681, 4590, 260, 138)$$

X, Y, and Z are then converted to RGB values by[3]:

$$\begin{pmatrix} R \\ G \\ B \end{pmatrix} = \begin{pmatrix} 3.24096994 & -1.53738318 & -0.49861076 \\ -0.96924364 & 1.8759675 & 0.04155506 \\ 0.05563008 & -0.20397696 & 1.05697151 \end{pmatrix} \begin{pmatrix} X \\ Y \\ Z \end{pmatrix}$$

Gamma correction was applied by the below function, to the values of R, G, and B:

$$\gamma(u) = \begin{cases} \frac{323u}{25} & u \leq 0.0031308 \\ \frac{211u^{5/12} - 11}{200} & otherwise \end{cases}$$

As for the temperature of the accretion disk, it is proportional to a function of radius r and the inner radius r_i:[4]

$$T \sim r^{-3/4}(1 - \sqrt{r_i/r})^{1/4} \qquad \textbf{Equation 3.}$$

3 COMPUTATIONAL METHODS

3.1 *Trajectory of photon*

From **Equation 1**, the inverse of the radial distance $u = 1/r$ of a photon can be numerically computed at intervals of $h = \pi/1800$ rad through the improved Euler's method, with the first derivative $du/d\theta = u'$ computed through the basic Euler's method.

$$
\begin{aligned}
u'_{n+1} &= u'_n + h\left(\frac{3GMu_n^2}{c^2} - u_n\right) \\
u_{n+1} &= u_n + h\frac{u'_n + u'_{n+1}}{2} \\
&= u_n + h\frac{2u'_n + h(\frac{3GMu_n^2}{c^2} - u_n)}{2}
\end{aligned}
$$

With the camera is placed a distance $r = 100r_s$ from the origin, on the z-axis, the initial conditions are $u_0 = 1/100r_s$, $\theta_0 = 0$, $u'_0 = u_0/tan(\theta_{in})$. θ_{in}, the initial angle of the trajectory w.r.t the z-axis, would depend on the position of the pixel on the camera.

The trajectory is stored as an array of values for r, $dr/d\theta$ at intervals of h, to allow later retrieval of these values needed in other computation.

3.2 *Creating an image*

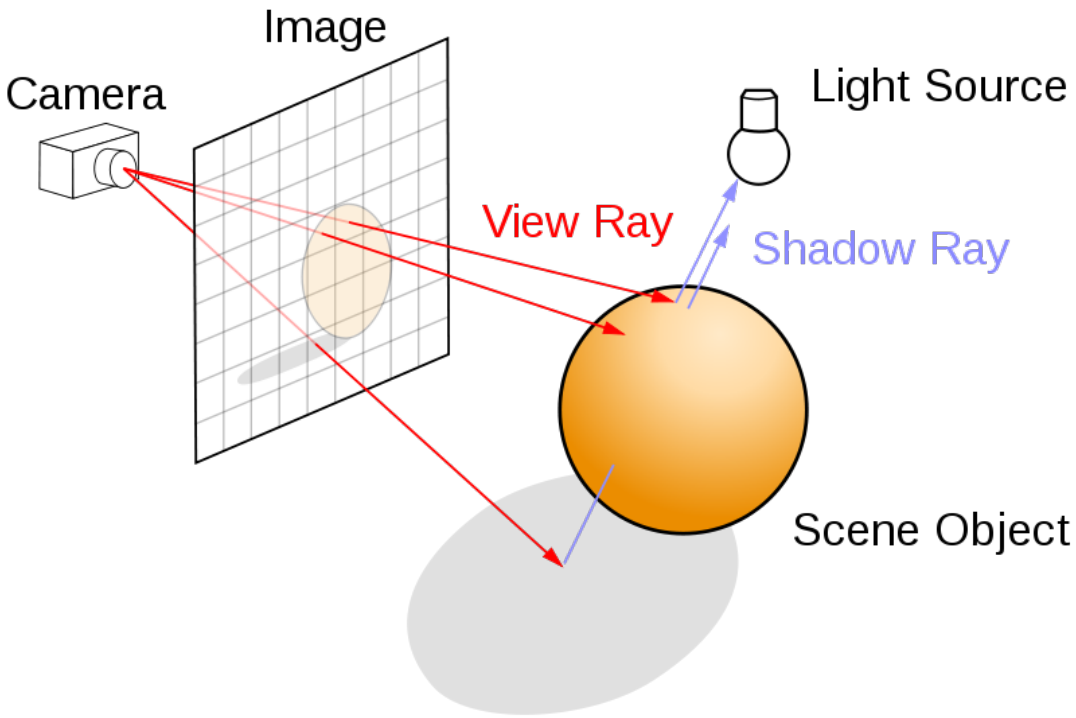

Figure 1. How raytracing creates an image. Image in Wikimedia commons.

From a camera at a point, an image is created by tracing the path of light at particular polar and azimuthal angles determined by the position of a pixel, and colouring the pixel depending on where the path of light terminates. For an image with a field of view (fov) angle ψ, number of horizontal pixels n_h, the angle θ_{in} subtended by the i^{th} vertical and j^{th} horizontal pixel from the centre of the image will be given by:

$$\theta_{\text{in}} = \arctan\left(\frac{\sqrt{(2i-1)^2+(2s-1)^2}}{n_h} * tan\left(\frac{\psi}{2}\right)\right)$$

To reduce the computation required, we may exploit certain symmetries in the system. Considering the radial symmetry of the above equation for the array of pixels, for each i, j within the central square of pixels, there will be 7 other pixels that will have the same θ_{in}. Outside of the central square of pixels, likewise, there will be 3 other pixels that will have the same θ_{in} for any particular pixels. This is illustrated below for an example 8x10 array:

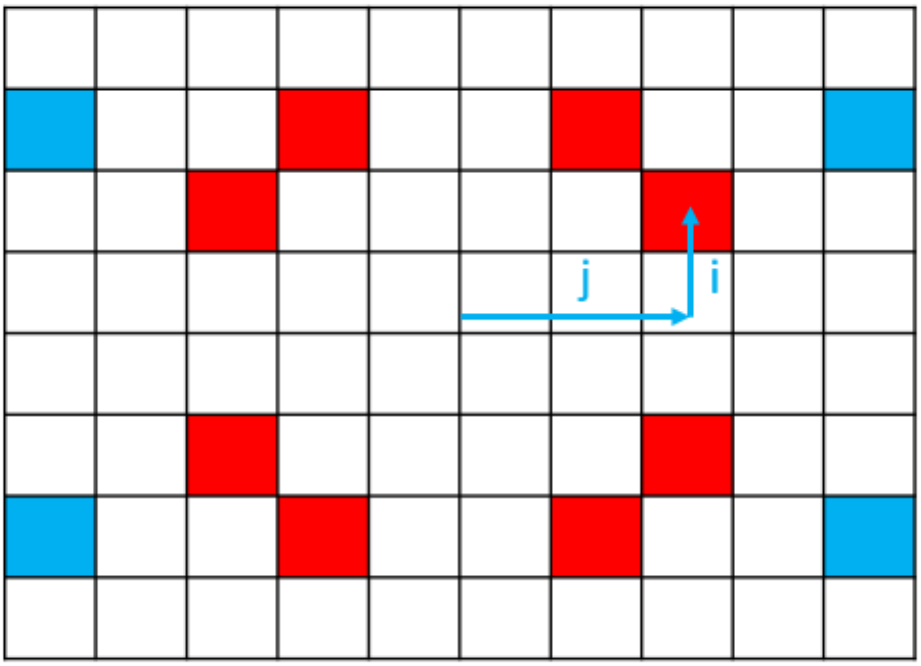

Figure 2. The 8 pixels highlighted in red will produce the same θ_{in}. Similarly, the 4 pixels highlighted in blue will also produce the same θ_{in} as each other.

As such, the same trajectory will be produced for all 8 pixels within the central square (4 if outside central square), albeit at different azimuthal angles. By generating the trajectory as sets of $(r, dr/d\theta)$ at intervals of $h = pi/1800$, we just need to check the values of r at values of θ where the accretion disk is expected to be for the particular azimuthal angle of each pixel. This greatly reduces the number of trajectories that need to be computed.

Considering the parameterisation of the disk from section 2.2, the polar angle of the disk at azimuthal angle ϕ for a disk inclined at α can be found by (a derivation can be found in **appendix A**):

$$\theta_{\text{disk}} = \begin{cases} -\arctan\left(\frac{1}{\cos(\phi)\tan(\alpha)}\right) & \pi/2 \leq \phi \leq 3\pi/2 \\ \pi - \arctan\left(\frac{1}{\cos(\phi)\tan(\alpha)}\right) & \text{otherwise} \end{cases}$$

Having the top of the image as $\phi = 0$, increasing anti-clockwise. For each pixel, we need to check if $3r_s \leq r \leq 10r_s$ at θ_{disk}. Considering that our values of r are in intervals of $h = \pi/1800$ rad, we use a linear Langrange interpolation to get a more accurate value rather than just taking r at the closest value of θ:

$$r = \frac{(1 - (\theta_{\text{disk}} - \theta_n))}{h} r_n + \frac{(\theta_{\text{disk}} - \theta_{n+1})}{h} r_{n+1}$$

Where $\theta_n \leq \theta_{\text{disk}}$ and $\theta_{\text{disk}} \leq \theta_{n+1}$. As some light rays may miss the disk for the first value θ_{disk} and intersect the disk at $n\pi + \theta_{\text{disk}}$, where n is a positive integer, our trajectories are plotted for $\theta \in [0, 4\pi]$. An example would be rays that bend to hit the disk behind the black hole, or rays near the photon sphere that make a complete revolution before hitting a part of a disk. The values of r are then at $n\pi + \theta_{\text{disk}}$, if it does not intersect the disk at $(n-1)\pi + \theta_{\text{disk}}$.

Lastly, to save on computation, the tracing the trajectory is terminated if it goes within the photon sphere at $r < 1.5r_s$, as well as if it reaches a distance $r > 2r_{\text{disk}}$ beyond $\theta > \pi/2$.

3.3 *Determining the colour of a pixel*

For the aforementioned termination conditions, a pure black colour is assigned to the pixel if its trajectory goes within the photon sphere, and a faint grey colour if it misses both the disk and the photon sphere.

The temperature of the disk in each image is specified by a specific temperature at the outermost radius, and allowed to vary as per **Equation 3** from section 2.4. As the temperature depends on r, and the redshift depends on both r and $dr/d\theta$ of the light ray at the disk (as per **Equation 2**from section 2.4), both these values are retrieved from the computed trajectory to use in the relevant equations. The temperature and redshift factor are computed as per the equations, with the notable exception that $v = -\sqrt{GM/(r - r_s)}$ when n is odd when intersecting the disk at $\theta = n\pi + \theta_{\text{disk}}$, as the ray would approach the disk from the back in such cases.

To determine the colour of a pixel whose trajectory intersects the disk, we use the integrals from section 2.4. Instead of converting the improper integrals by $\lambda = 1/(1-y)$, we observe that the colour matching functions are mostly bounded by [300nm, 800nm]:

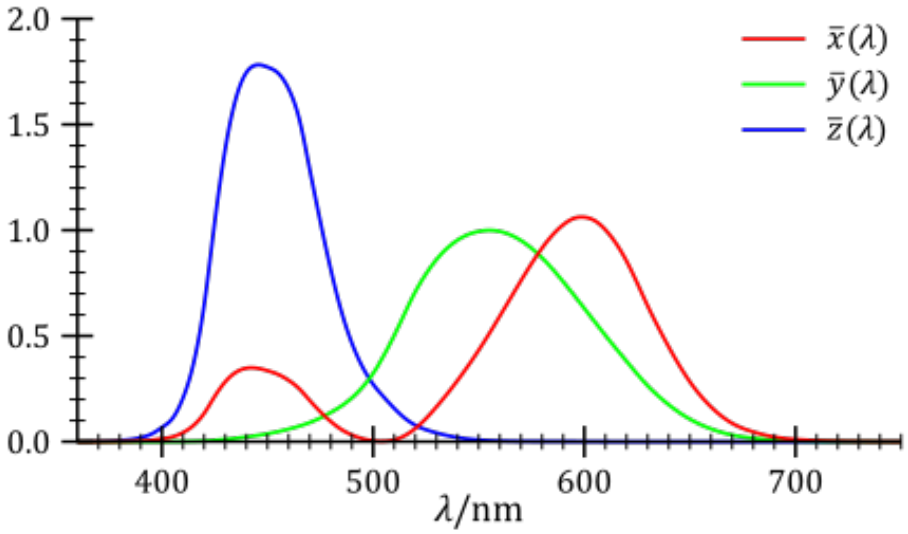

Figure 3. Plots of each colour matching function. Image in Wikimedia commons.

Thus, the composite Simpson's 1/3 rule was used to numerically compute the integrals at 1000 intervals over [300nm, 800nm], to obtain X, Y, and Z. These are then converted to RGB values, which are then normalized such that only 5% of the RGB values are saturated, to be able to visually discern differences in colour and brightness in the images produced.

4 RESULTS

Following are the rendered images from the algorithm, at $r_{\text{camera}} = 100r_s$, and number of pixels corresponding to full HD specifications (1920×1080). Images with inclination at $\alpha = 80°$ has fov angle $\phi = \pi/14$, and images with inclination at $\alpha = 30°, 60°$ has fov angle $\phi = \pi/11$.

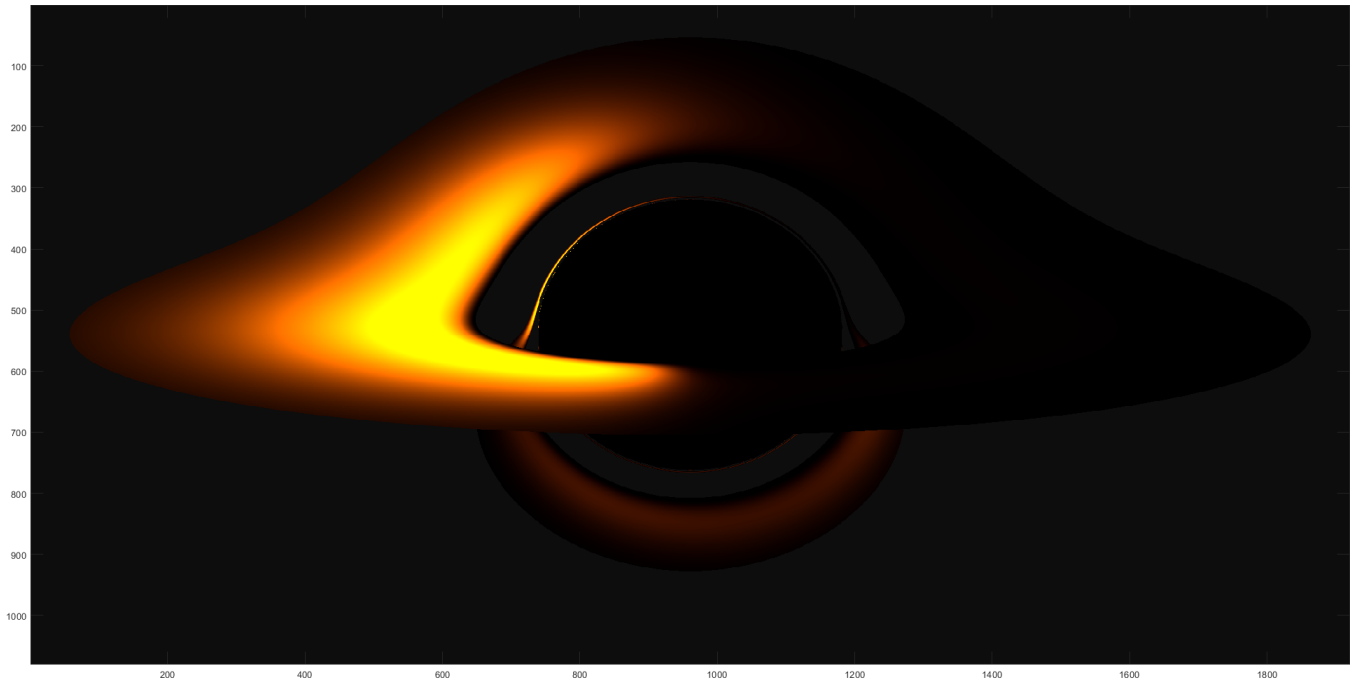

Figure 4. Image with $T_{\text{outer}} = 1000K$, inclination $\alpha = 80°$.

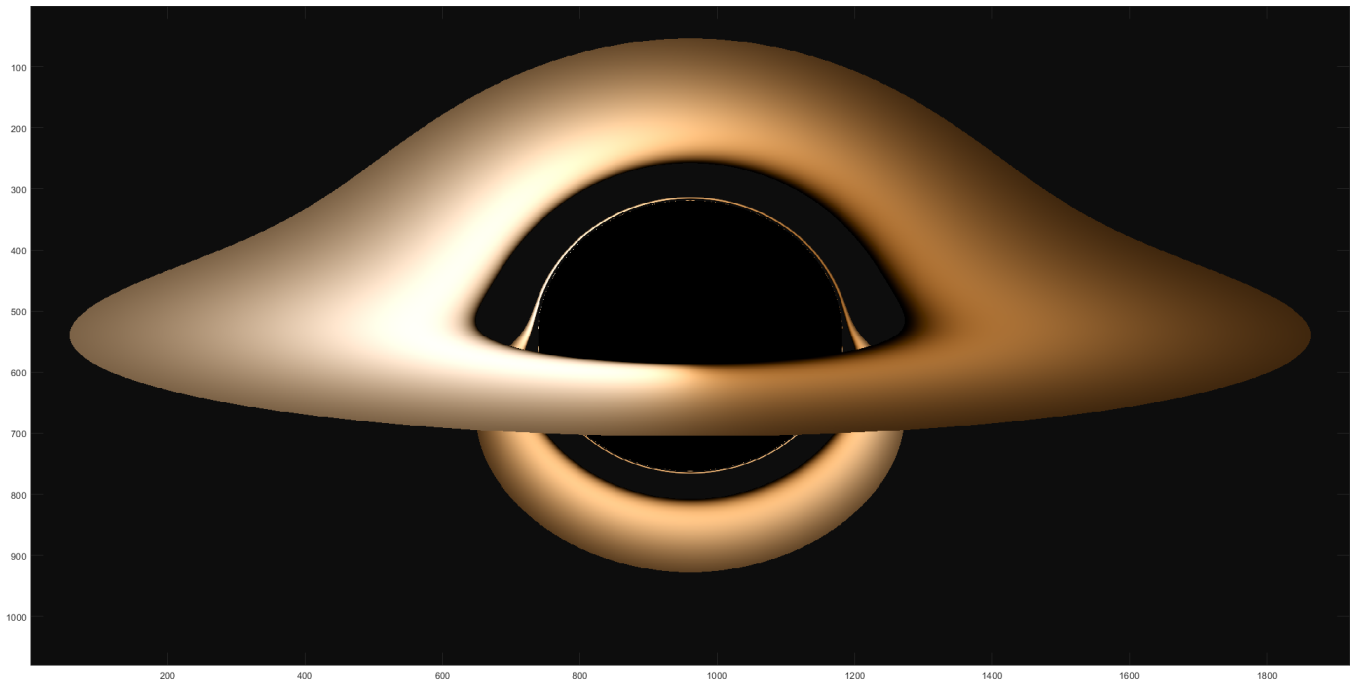

Figure 5. Image with $T_{\text{outer}} = 3000K$, inclination $\alpha = 80°$.

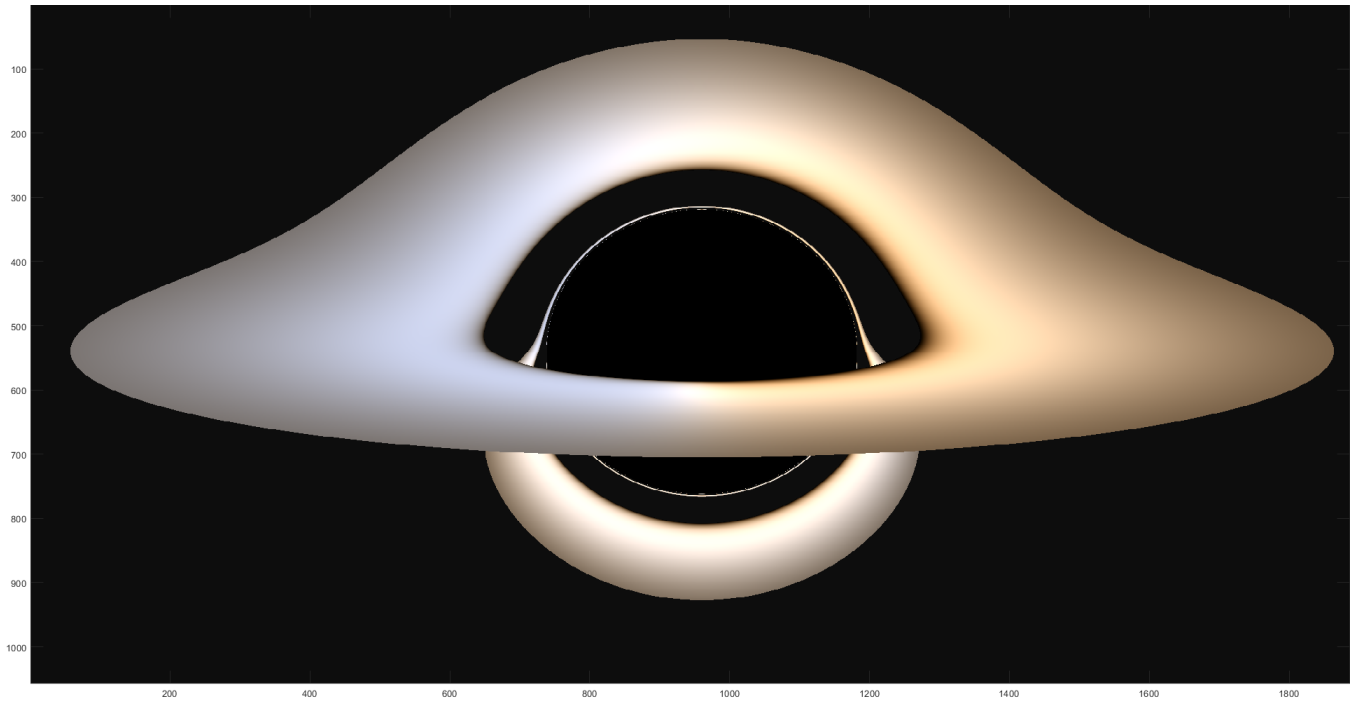

Figure 6. Image with $T_{\text{outer}} = 5000K$, inclination $\alpha = 80°$.

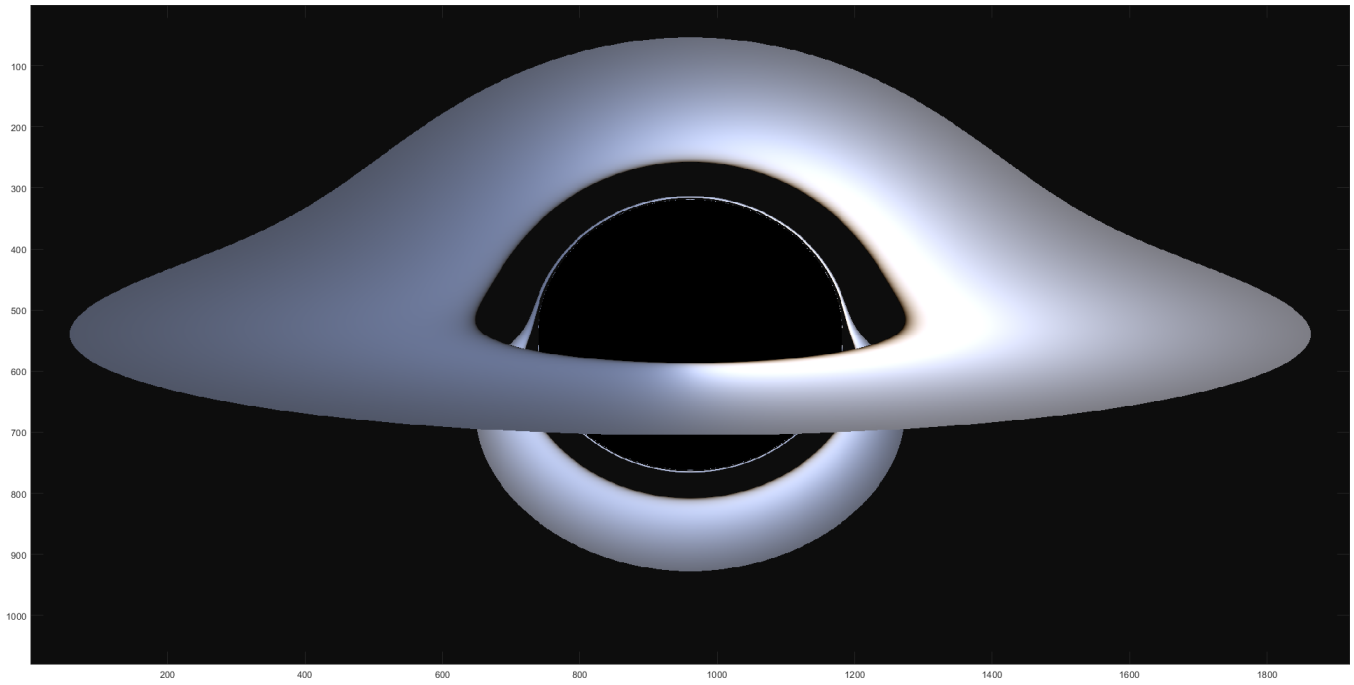

Figure 7. Image with $T_{\text{outer}} = 10000K$, inclination $\alpha = 80°$.

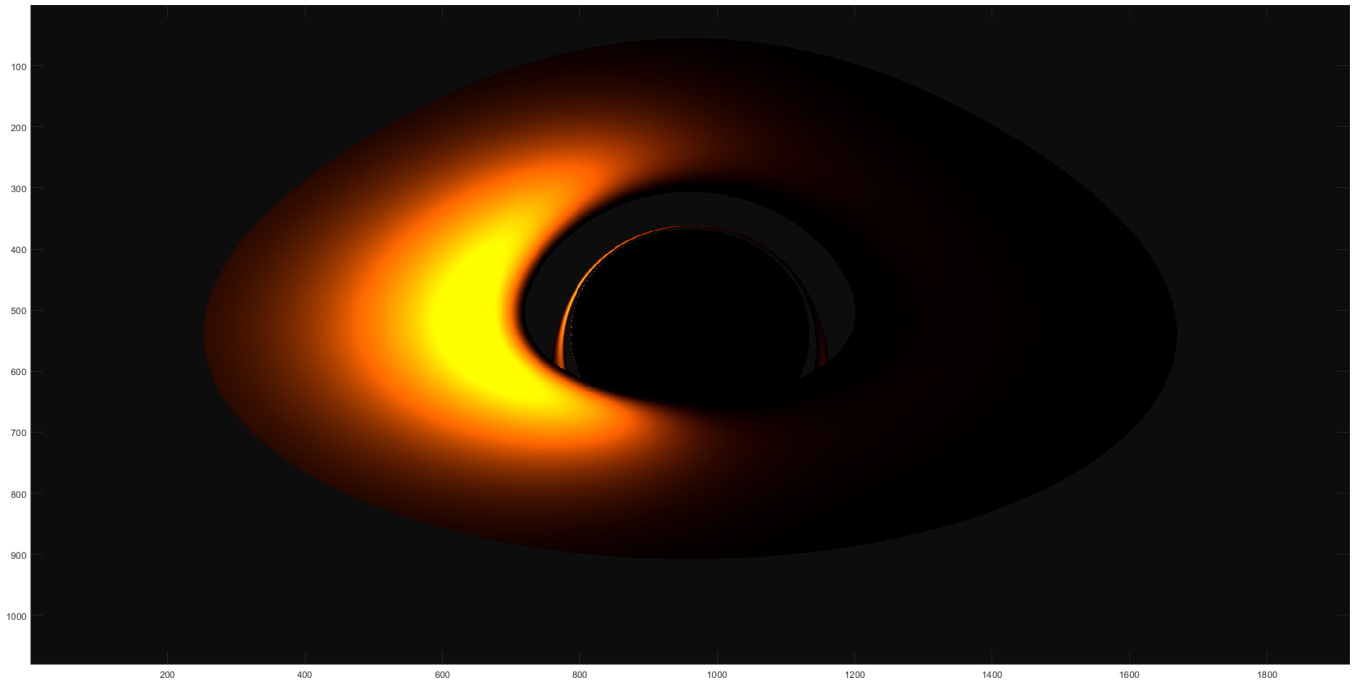

Figure 8. Image with $T_{\text{outer}} = 1000K$, inclination $\alpha = 60°$.

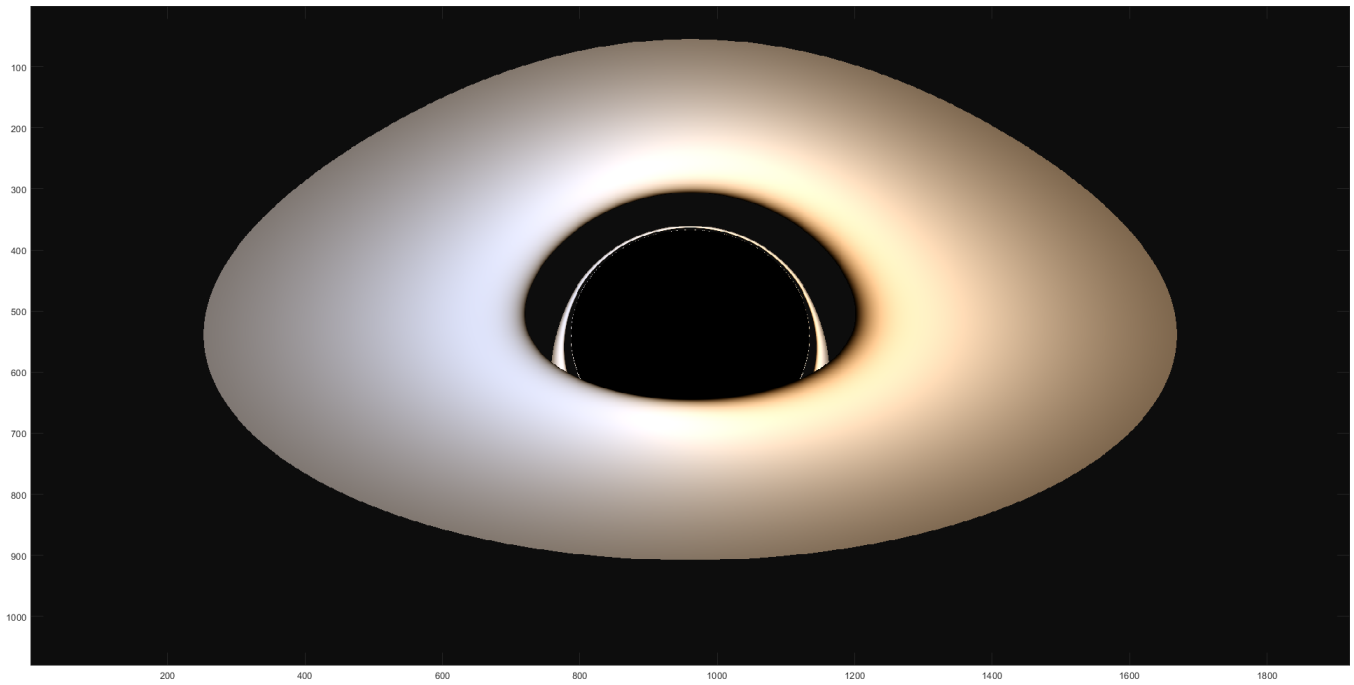

Figure 9. Image with $T_{\text{outer}} = 5000K$, inclination $\alpha = 60°$.

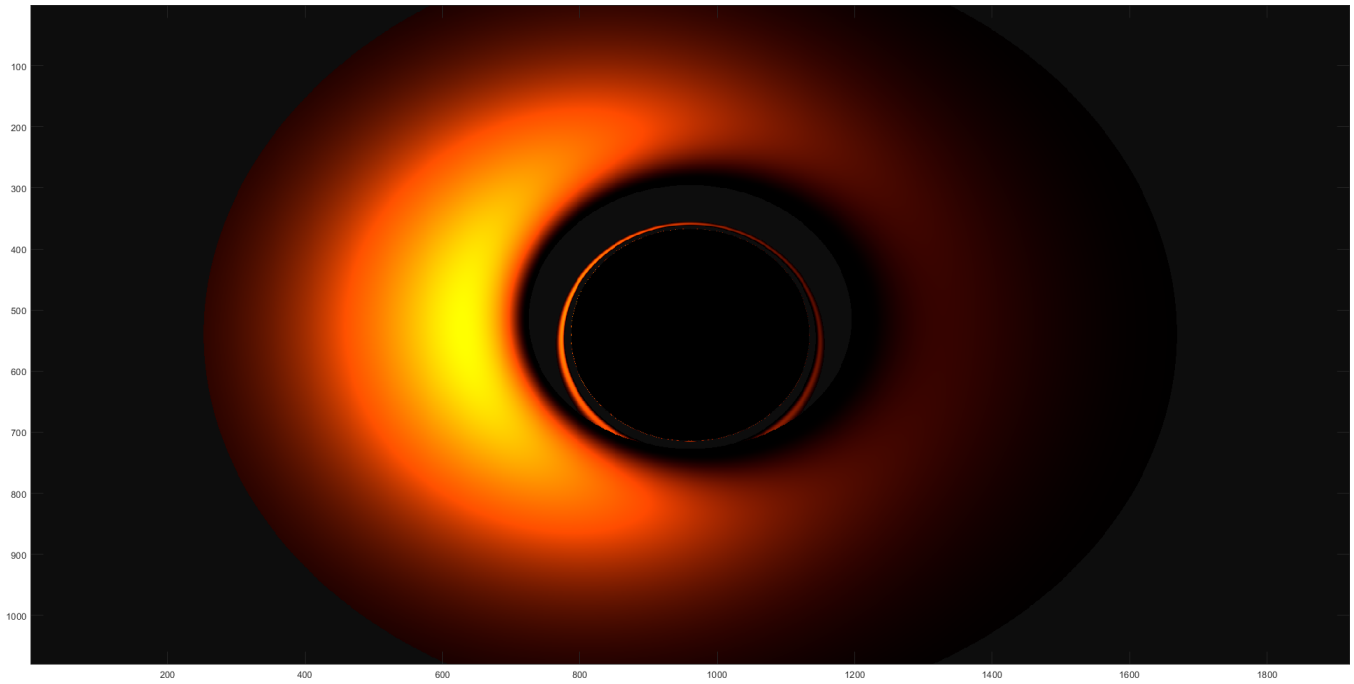

Figure 10. Image with $T_{\text{outer}} = 1000K$, inclination $\alpha = 30°$.

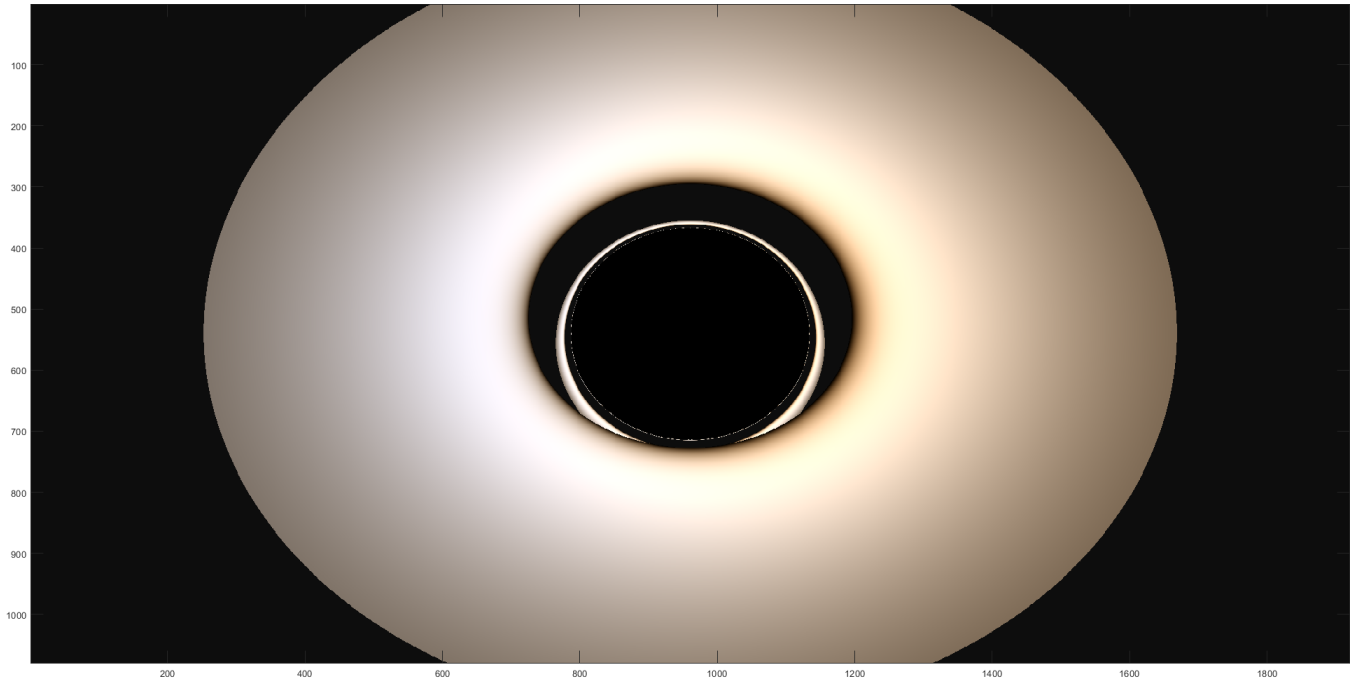

Figure 11. Image with $T_{\text{outer}} = 5000K$, inclination $\alpha = 30°$.

5 DISCUSSION

The full HD images are able to be rendered within 30 minutes on my personal desktop built 7 years ago, which is a reasonable speed.

The image of the posterior portion of the disk is able to be seen both above and below the black hole. Furthermore, the strongly warped trajectories that pass close to the photon sphere is able to be observed, manifesting as a thin ring around the photon sphere, corresponding to trajectories that eventually hit the accretion disk. This corresponds well to prior research done in black hole modelling. As a example of prior work, below is an image of the black hole in the movie *Interstellar*, which is rendered via similar raytracing methods as described in this paper (James *et al.*, 2015)[5], albeit for a Kerr (spinning) black hole, with a diffuse accretion disk:

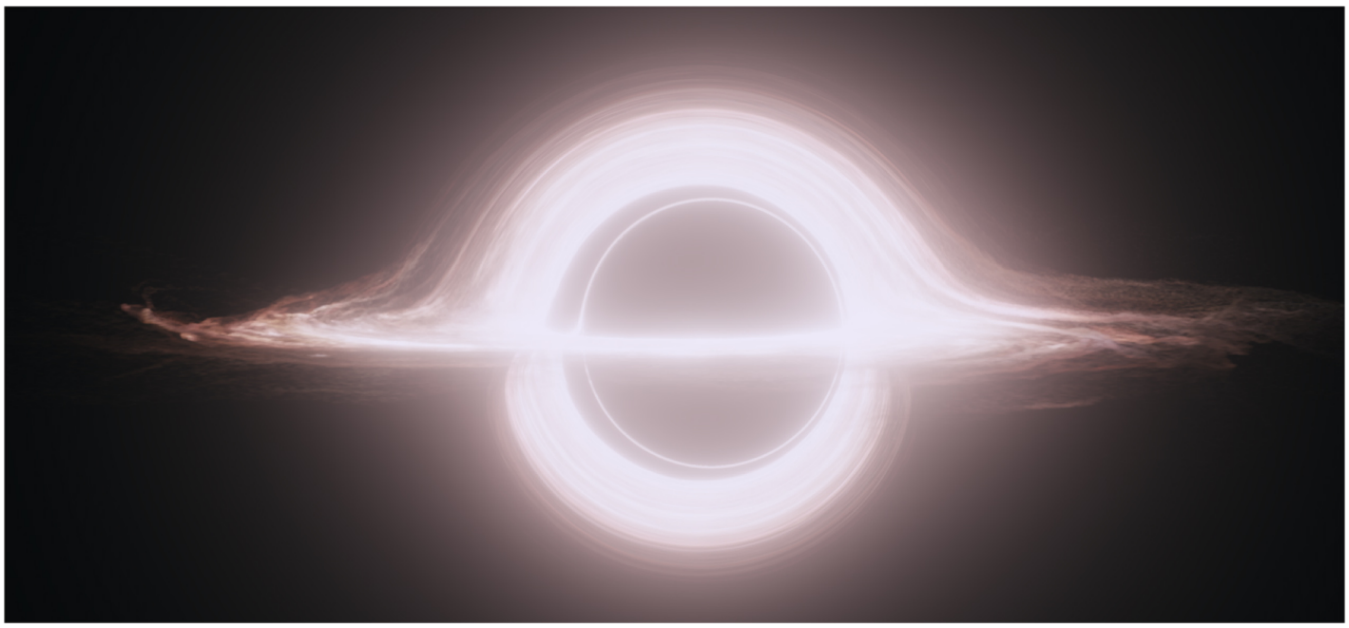

Figure 12. Digital image of Kerr black hole with diffuse accretion disk, variant of the accretion disk seen in *Interstellar*. (Credit: James *et al.* & Warner Bros. Entertainment Inc.)[5]

In our produced images, it can be observed that portions of the disk approaching the camera (left side of images) will be blueshifted due to the doppler effect, and portions of the disk moving away (right side of images) are redshifted. In addition, at greater inclinations, the effect of doppler red/blueshift decreases as intended.

As another comparison, below is the image of the supermassive black hole at the center of the M87 galaxy, observed by the Event Horizon Telescope collaboration, 2017[6]. It can be observed that the lower portion of the accretion disk has a higher intensity due to relativistic beaming:

Figure 13. Observed image of M87 galaxy quasar. Colour depicts intensity of EM radiation at wavelength $\lambda = 1.3mm$, rather than true colour. Credit: Event Horizon Telescope collaboration *et al.*[6]

One bug encountered during production was the appearance of the erroneous lines as highlighted in the below image:

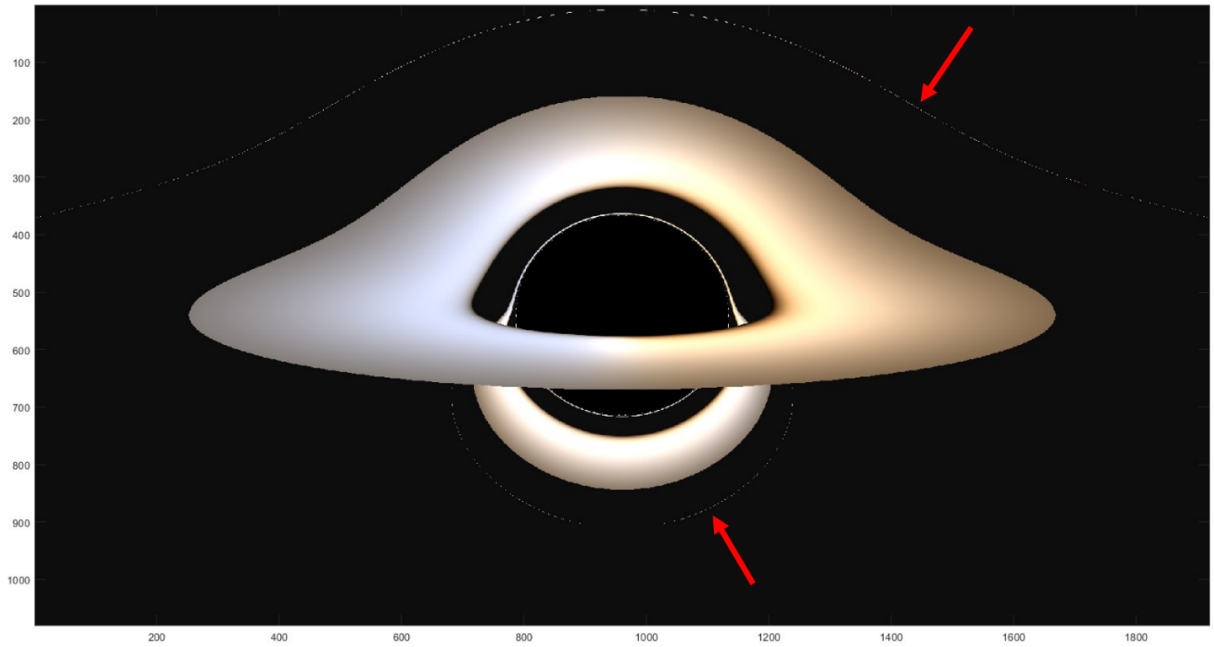

Figure 14. Rendered image with erroneous lines

It did not make physical sense that trajectories at θ_{in} greater than those that intersect the disk with

minimal warping would intersect the disk too. Through plotting the trajectory of one such line, it was discovered that the linear Lagrange interpolation caused the issue in combination with terminating the trajectory when $r > 2r_{\text{disk}}$. The latter would have the effect of setting r_{n+1} to be `0` in the interpolation, thus causing the produced r to be $3r_s \leq r \leq 10r_s$, as if the trajectory intersected the disk. This was remedied by having the trajectory be determined to miss the system when $r_n = 0$ or $r_{n+1} = 0$.

6 CONCLUSION

Given the rendered images correspond well to what is currently known, it is likely the algorithm was implemented correctly. Possible improvements may include the vectorisation of the functions used to calculate the trajectories and produce color, which currently take up most processing time.

APPENDIX A

The plane on which the accretion disk lie has the equation:

$$\hat{n} \cdot \begin{pmatrix} x \\ y \\ z \end{pmatrix} = 0$$

Where $\hat{n}$ is a vector normal to the disk, which can be found as the cross product of two linearly independent vectors on the disk. From the equation describing the disk from section 2.2, two orthonormal vectors can be found with $\phi = 0$ and $\phi = \pi/2$. $\hat{n}$ can be found:

$$\begin{aligned} \hat{n} &= \begin{pmatrix} \cos\alpha \\ 0 \\ -\sin\alpha \end{pmatrix} \times \begin{pmatrix} 0 \\ 1 \\ 0 \end{pmatrix} \\ &= \begin{pmatrix} \sin\alpha \\ 0 \\ \cos\alpha \end{pmatrix} \end{aligned}$$

Thus, $x\sin\alpha + z\cos\alpha = 0$ on the plane. Substituting in x and z in spherical coordinates,

$$\begin{aligned} r\sin\theta\cos\phi\sin\alpha &= -r\cos\theta\cos\alpha \\ \tan\theta &= -\frac{\cos\alpha}{\cos\phi\sin\alpha} \\ \theta &= -\arctan\left(\frac{1}{\cos\phi\tan\alpha}\right) \end{aligned}$$

Considering the disk has $\theta_{\text{disk}} > \pi/2$ when $\pi/2 \geq \phi$ or $\phi \geq 3\pi/2$, and arctan has range $(-\pi/2, \pi/2)$, we get:

$$\theta_{\text{disk}} = \begin{cases} -\arctan\left(\frac{1}{\cos(\phi)\tan(\alpha)}\right) & \pi/2 \leq \phi \leq 3\pi/2 \\ \pi - \arctan\left(\frac{1}{\cos(\phi)\tan(\alpha)}\right) & \text{otherwise} \end{cases}$$

REFERENCES

1. Carroll, Sean M. (December 1997). "Lecture Notes on General Relativity: The Schwarzschild Solution and Black Holes". arXiv:gr-qc/9712019. Bibcode:1997gr.qc....12019C. Retrieved 2021-03-24
2. CIE 1931 color space. (2021, March 18). Retrieved March 24, 2021, from https://en.wikipedia.org/wiki/CIE_1931_color_space
3. Michael Stokes; Matthew Anderson; Srinivasan Chandrasekar; Ricardo Motta (November 5, 1996). "A Standard Default Color Space for the Internet - sRGB, Version 1.10"
4. Spruit, H. C. (n.d.). Accretion Disks. Lecture. Retrieved March 24, 2021, from https://wwwmpa.mpa-garching.mpg.de/ henk/pub/disksn.pdf
5. James, O., Tunzelmann, E. V., Franklin, P., &; Thorne, K. S. (2015). Gravitational lensing by spinning black holes in astrophysics, and in the movie interstellar. Classical and Quantum Gravity, 32(6), 065001. doi:10.1088/0264-9381/32/6/065001
6. Akiyama, K., Alberdi, A., Alef, W., Asada, K., Azulay, R., Baczko, A., . . . Ziurys, L. (2019). First M87 event Horizon Telescope Results. I. the shadow of the supermassive black hole. The Astrophysical Journal, 875(1). doi:10.3847/2041-8213/ab0ec7